Vol.9 No.2
Spring 1998

PERFORMANCE OF AB_2 ALLOYS FOR HYDROGEN STORAGE AND HYDRIDE ELECTRODES

A. A. Rostami[1]*, K. Petrov[2] and S. Srinivasan[2]

[1] *Institute of Chemistry, Mazandaran University, Babolsar, Islamic Repbulic of Iran*
[2] *Center for Electrochemical Systems and Hydrogen Research,Texas Engineering Experiment Station, Texas A& M University System, College Station, TX 77843 -3402 U.S.A*

Abstract

Two types of hydride electrodes are potential candidates to replace the Cd electrode in Ni|Cd batteries. One is of the AB_5 type where A is a rare earth metal or mixture thereof, and B is the transition metal. The other is commonly referred to as AB_2 type. AB_2 type alloys with partial substitution of the B element in AB_2 type hydride material (Ovonic) with Co, Mn, Al, and Fe were studied (A components were Ti and Zr, the major B components were V, Ni, and Cr). The materials were prepared by arc melting and characterized using X-ray diffraction and SEM techniques. The hydrogen absorption|desorption pressure-composition isotherms for the alloys were determined. Partial substitution of the B element changes the initial, multiphase structure of the basic composition. Mn increases the plateau pressure, while addition of small amounts of Al and Fe have positive influence. Generally, the addition of described elements does not improve the characteristics of the basic material (Ovonic). The electrochemical storage capacities of based system were in the range of 300-400 mAh/g.

Introduction

Nickel-hydrogen batteries using hydrogen storage alloys have attracted much attention because they have inherent advantages over conventional secondary batteries with respect to discharge capacity, cleanliness and tolerance to overcharge and overdischarge. Intensive research on reversible hydrogen absorbing alloys for hydride electrodes has led to the development and applications of rechargeable nickel/metal hydride batteries. These compact, sealed batteries have higher energy densities than those of nickel-cadmium batteries [1-2]. Typical AB_2 laves phase systems are being evaluated in our laboratories [3]. In this study, modifications of the composition of the parent V-Ti-Zr-Ni systems are being made with different additive elements to optimize their thermodynamic properties and increase the hydrogen storage capacity.

The role of specific elements in AB_2 type alloys can be summarized briefly as follows: Ti, Zr, V are hydrogen storage elements. Ti and Zr form thick, dense, passive oxides in alkaline solution, while V forms easily soluble oxide, which is important for activation and increasing porosity on the surface; Zr provides a controllable degree of embrittlement to the metal; Ni adjusts M-H bond strength and is a catalyst for hydrogen/hydroxyl reaction; Cr inhibits

Keywords: Charge and discharge capacity; Metal hydride electrodes; Rechargeable batteries

* Author to whom correspondence should be addressed

the unrestrained corrosion of vanadium [4-6]. Available information on the cycle life of Ni/MH_x cells appears to indicate that an AB_2 type alloy developed by the Ovonic Battery Company shows a considerably longer cycle life (>800 cycles at 100% depth-of-discharge)[7] than an AB_5 type alloy.

It has been claimed that alloys with a composition of $Ti_{16}Zr_{16}V_{22}Ni_{39}Cr_7$ ($A_{32}B_{61}Cr_7$) and $Ti_{16}Zr_{15}V_{31}Ni_{32}Cr_7$ ($A_{31}B_{63}Cr_7$) are promising for a Ni/MH_x cell [8]. In this work we have tried to improve these compositions by partial substitution of the B element with Co, Mn, Al, and Fe. Substitution of Ni with Co in $LaNi_5$ showed substantial improvements [9-10], thus it may be worth investigating the incorporation of Co in AB_2 type alloys also. The reason for investigating a Fe additive is that this metal is in the same group as Co on the periodic table. These metals are also compatible with the nickel electrode in a Ni/MH_x battery. Mn or Al is interesting as a minor component (Mm $Ni_{3.6}Mn_{0.4}Al_{0.4}Co_{0.7}$, where Mm denotes misch metal) because these elements showed substantial improvement for $LaNi_5$ type alloys [9-10].

Experimental Section

Samples were prepared by arc melting the constituent elements into ingots in an argon atmosphere, followed by annealing for three days at 800°C. The ingots were crushed, ground mechanically and passed through sieves to produce a powder of 100 mesh. The crystalline characteristics and lattice constants were determined by X-ray diffraction patterns. Analysis of the composition and distribution of the elements were determined using a J. S. M. model 6400 Scanning Electron Microscope equipped with a NORAN I-2 EDX unit and SEM/EDS techniques.

Gas phase hydrogen absorption/desorption capabilities of the alloys, as well as their hydrogen content, were measured using a modified Sievert's type apparatus. Absorption/desorption isotherms were generally carried out at room temperature on preactivated samples to determine the P-C isotherms by equilibrating the solid hydride-phase by the addition or withdrawal of measured increments of ultra pure hydrogen gas in the reactor. The amount of hydrogen (gram atom) absorbed/desorbed by the various alloys, and thus the H/Mol (the amount of hydrogen absorbed per mole of alloy) ratios in the P-C plots, were calculated from the ideal gas P-V-T relation which translates in terms of transducer ("Dynisco") readings to: [11]

$$H = 2\nu\,\Delta P/RT - \Sigma c \equiv 2\nu\,\Delta t\varphi / RT - \Sigma c \qquad (1)$$

where R and T have their usual meanings, ν is the volume of reservoir, φ is the slope of the pressure versus transducer reading curve, Δt is the change in transducer reading, and Σc is a correction factor accounting for hydrogen in the gaseous phase in equilibrium with the solid hydride phase. From P-C-T curves it is easy to estimate the electrochemical unit for hydrogen capacity-(mAh/g. HM), because each absorbed/desorbed hydrogen atom corresponds to the transfer of one electron. When a fully charged electrode is electrochemically discharged, the discharge capacity, C_d, is thus interrelated to the gram-atom of hydrogen absorbed, (x), via the equation:

$$C_d\,(mAh/g) = xF/3.6\,W_M \qquad (2)$$

where F and W_M are, respectively, Faraday's constant and the molecular weight of the electrode material and x is the number of hydrogen atoms per alloys molecule.

Electrochemical hydrogen storage capabilities of the alloys were monitored by measuring the corresponding charge/discharge characteristics in 8 M (31%) KOH solution by application of desired current using Solartron-1286 Electrochemical Interface. Test electrodes were prepared by mixing well 75 mg alloy particles with an appropriate amount of Teflonized carbons, or Teflonized acetylene black-XC-35 [3], which act as a binder, and loaded in a porous nickel current collector (1 cm^2), followed by cold pressing at 300 kg/cm^2. A three electrodes, one compartment Teflon cell containing 31% KOH electrolyte solution was employed for measuring electrode capacity, cycle life, rate capabilities and charge-retention. The reference electrode was Hg/HgO/31% KOH. The test electrodes were activated by continuous galvanostatic cycling until a constant value of the hydrogen capacity was obtained. In all electrochemical tests, the cut-off potential was 0.8 V versus the Hg/HgO reference.

Results and Discussion

X-Ray Diffraction and SEM/EDS Studies

Metal hydride alloys of the $Ti_{17}Zr_{16}V_{22}Ni_{39}Cr_7$ based system have been investigated in this project. The elements

Table 1. Alloy composition (AB_{2+x})

Elements	Additive	Sample I.D.
(Ti Zr Ni V Cr)		BNL-4
(Ti Zr Ni V Cr)	Mn Co	BNL-9
(Ti Zr Ni V Cr)	Mn Co	BNL-11
(Ti Zr Ni V Cr)	Mn Co	BNL-13
(Ti Zr Ni V Cr)	Al Co Fe	BNL-10
(Ti Zr Ni V Cr)	Mn Al Co Fe	BNL-12

added to this based system to prepare new compositions and their sample identification are listed in Table 1.

The metal hydride alloys were then examined by X-ray diffraction (XRD) and energy dispersive spectrometer (EDS). Qualitative (EDS) analysis of the samples revealed compositions that were close to the starting elemental combinations. Table 2 shows the lattice parameters exhibited by these alloys.

P-C Isotherms

The pressure-composition-temperature (P-C-T) curve of the metal hydride is one of the important factors affecting cell internal pressure. A large amount of hydrogen absorption is desirable within certain limits of hydrogen equilibrium pressure, that is, from 1.0 atm to 0.01 atm. Below the level of 0.01 atm, hydrogen has a strong bond strength with metal. At high rates or low temperatures, the discharge is limited because of slow hydrogen diffusion in bulk. Above the level of 1.0 atm, hydrogen tends to have an unstable bond with metals which causes a higher rate of self discharge in the batteries. Thus, the effective capacity can be determined from the composition range (hydrogen/formula unit, i.e. H/AB_2 ratio), which lies within these pressure limits. Figure 1 shows a family of absorption isotherms at 25°C for all tested alloy compositions (BNL-4, BNL-9, BNL-10, BNL-11, BNL-12, BNL-13). The P-C isotherms show bigger differences than expected from slight changes in the composition of the alloys, especially BNL-11, 13. This could be due to the influence of parameters (processing, surface properties, etc.) different from the role of specific elements, making it difficult to draw definite conclusions [9]. Nevertheless, comparing BNL-10 (Mn-0.00), BNL-9 (Mn-0.08) and BNL-12 (Mn-0.16) we can say that Mn increases the plateau pressure, while the addition of small amounts of Al and Fe lower the equilibrium hydrogen pressure and yield a small higher

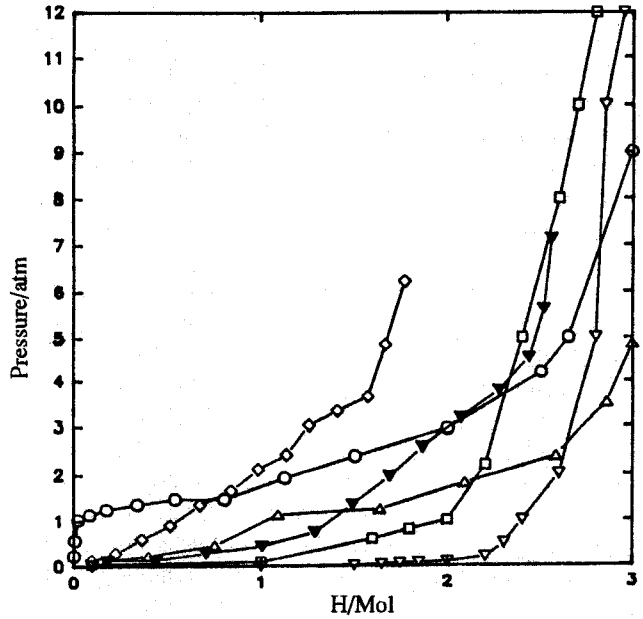

Figure 1. Pressure-composition absorption isotherms for: BNL-4; ▽, BNL-9; ▼, BNL-10; □, BNL-11; ○, BNL-12; △, BNL-13; ◇. at roomt temperature

hydrogen capacity (compare BNL-10, 12 versus BNL-9, 11, 13). These results might be attributed to the effect of Al and Fe on the solid solution phase [12]. Generally, the addition of all these elements does not improve the gas-phase characteristics of the basic material (Ovonic) BNL-4. The equilibrium dissociation pressures and hydrogen capacity of BNL-4 are better than others (P-C isotherm lies between 0.01 and 1 atm up to 2.45 H/M storage capacity). Figure 2 represents the P-C-T curves for BNL-4 at different temperatures. The plateau pressure of BNL-4 increases with increasing temperature as expected [2]. The curves

Table 2. Parameters of the tested (AB_{2+x}) alloys

Sample I.D.	Hydride material composition	Mol weight (g)	Lattice constant a, (A°)	Lattice constant c, (A°)	Cell volume $(A°)^3$
BNL-4	$Ti_{0.51}Zr_{0.49}V_{0.67}Ni_{1.18}Cr_{0.21}$	183.24	4.9595	8.0877	172.3
BNL-9	$Ti_{0.5}Zr_{0.5}V_{0.62}Mn_{0.08}Ni_{0.86}Co_{0.5}Cr_{0.2}$	190.0	4.9538	8.0588	171.3
BNL-10	$Ti_{0.5}Zr_{0.5}V_{0.66}Al_{0.04}Ni_{0.66}Co_{0.44}Fe_{0.2}Cr_{0.2}$	190.5	4.9412	8.0354	169.9
BNL-11	$Ti_{0.5}Zr_{0.5}V_{0.64}Mn_{0.2}Ni_{0.66}Co_{0.5}Cr_{0.2}$	191.76	4.9398	8.0341	169.8
BNL-12	$Ti_{0.5}Zr_{0.5}V_{0.64}Mn_{0.16}Al_{0.04}Ni_{0.66}Co_{0.44}Fe_{0.06}Cr_{0.02}$	223.96	4.9556	8.0609	171.4
BNL-13	$Ti_{0.5}Zr_{0.5}V_{0.8}Mn_{0.8}Ni_{0.66}Co_{0.46}Cr_{0.2}$	189.85	4.9664	8.0798	172.6

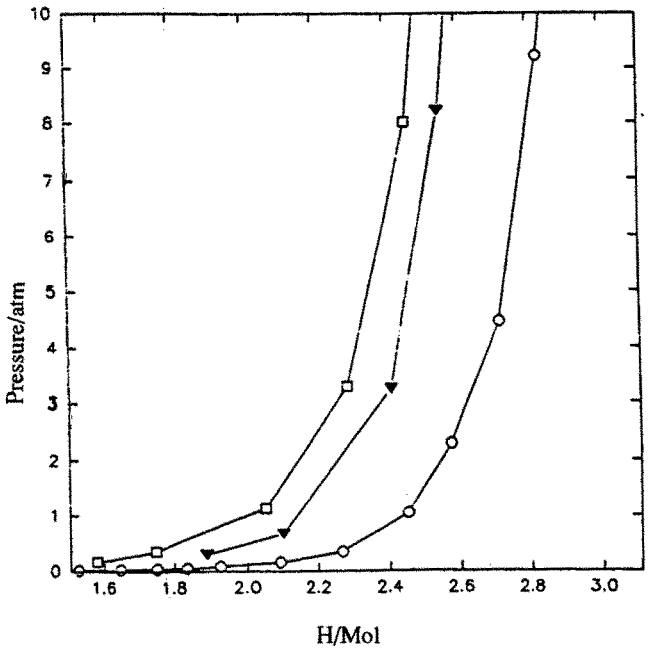

Figure 2. Pressure-composition absorption isotherms for BNL-4 at 20°C; ○, 40°C; ▼, 60°C; □

sloped, especially at higher temperatures, and have no flat plateaus.

In Table 3, all important gas-phase and electrochemical parameters of the tested alloys are summarized. The first two columns represent the gas-phase characteristics: (i) theoretical capacities; and (ii) hydrogen storage content up to 1 atm. equilibrium pressure. From these two parameters, the available hydrogen capacities in electrochemical units have been calculated using equation 2 which is shown in column three. As it follows from Figure 1, the BNL-4 alloy has a relatively wide plateau region, therefore, the value of capacity is quite large (350 mAh/g), that is compared to its theoretical value. In the case of other alloys, the capacity decreased to 71 mAh/g (BNL-13).

Electrode Capacity Measurements

Electrochemical absorption and desorption of hydrogen by a hydride material, M, incorporated in a test electrode, can be represented by the redox reaction:

$$M + xH_2O + xe^- \rightleftharpoons MHx + xOH^- \quad (3)$$

The specific electrochemical storage capacities, C_d, can be calculated from the amount of experimental electricity, Θ, discharged from the electrode, defined per weight of the hydride material in the electrode- W_{HM}:

$$C_d = \Theta / W_{HM} \ (mAh/g) \quad (4)$$

Electrochemical storage capacities of examined electrodes were obtained after repeated charge/discharge cycles using Vulcan-XC-72+PTFE and XC-35 (Teflonized acetylene black) as additives [3]. Figures 3 and 4 represent plots of capacity for BNL-10, BNL-12 and BNL-4 alloys as a function of the number of cycles, using a cut-off potential of 800 mV versus Hg/HgO at a rate of discharge 1/3C. From the curves it follows that these hydride materials need five to ten cycles to reach their plateau capacities, even though the powders were previously hydrided/dehydrided several times. The results for all materials are tabulated in Table 3. As Table 3 shows, it is obvious that BNL-4 has a superior electrochemical capacity, i.e. 320 mAh/g, in comparison to others with XC-35 additives.

The results for the three additives-Cu, acetylene black (XC-35) and Vulcan-XC-72+PTFE with BNL-4 are shown

Table 3. Properties of the (AB_{2+x}) hydride materials

Sample identification	Theoretical capacity mAh/g	Hydrogen content at 1 atm H/Mol	Capacity from P-C-T curves mAh/g	Electr. capacity additive (Vulcan +PTFE) mAh/g	Electr. capacity additive (XC-35) (mAh/g)
BNL-4	438	2.4	350	400	320
BNL-9	423	1.45	205	235	228
BNL-10	422	1.95	274	208	160
BNL-11	419	1.0	140	262	240
BNL-12	358	1.9	227	275	262
BNL-13	423	0.5	71	180	146

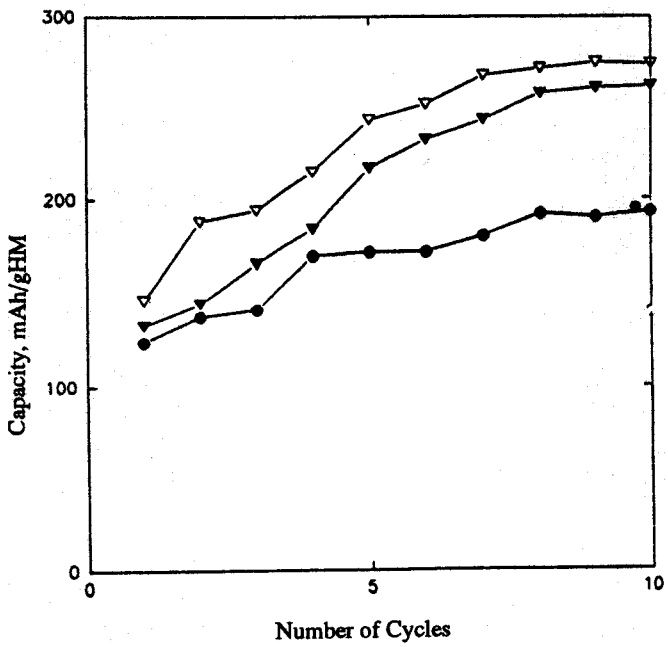

Figure 3. Discharge capacity versus cycle curves for: BNL-10 with Vulcan-XC-72+33% PTFE additive; ●, BNL-12 with XC-35 additive; ▲, BNL-12 with Vulcan-XC-72+33% PTFE additive, Δ.

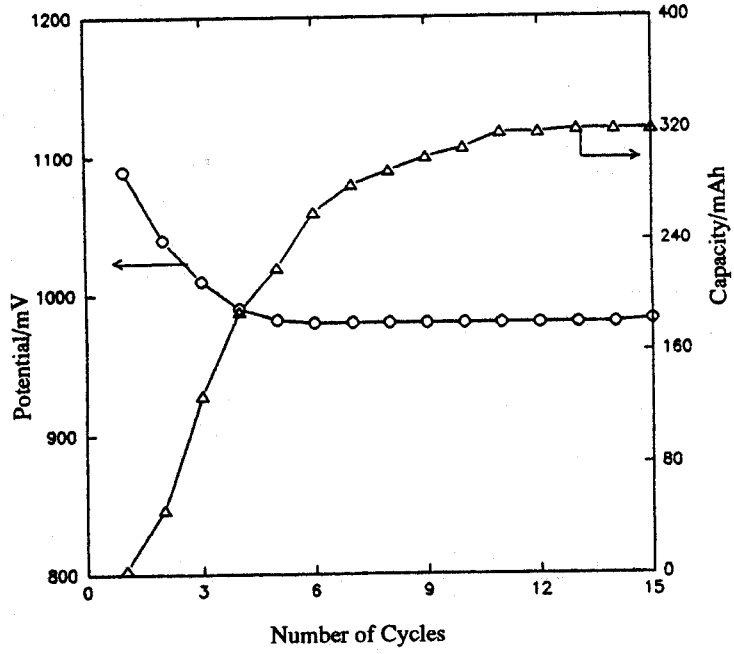

Figure 5. Potential at the end of charge and capacity versus number of cycles at C/3 charge-discharge for BNL-4 active material with XC-35 additive

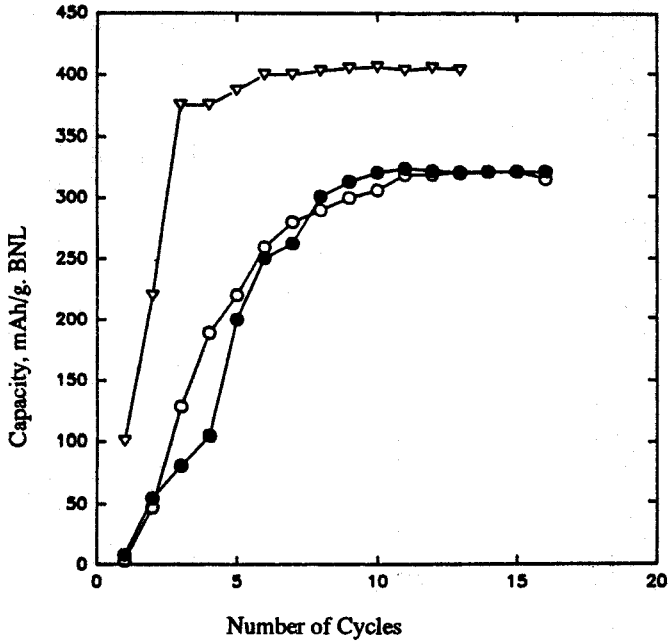

Figure 4. Discharge capacity versus cycle curves for BNL-4 with: Cu; ○, XC-35; ●, Vulcan-XC-72+33% PTFE additives; ▽.

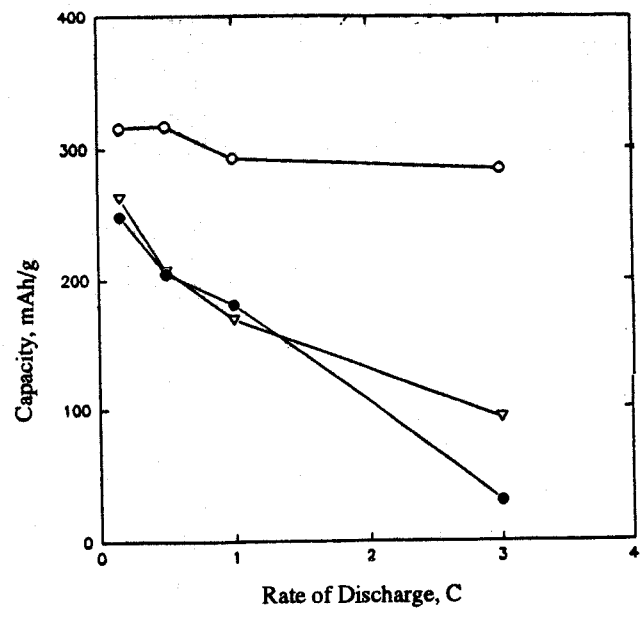

Figure 6. Discharge capacity versus discharge rate, C, for: BNL-4; ○, BNL-11; ●, BNL-12 with XC-35 additive; ▽.

in Figure 4. This figure shows that the maximum capacity of the electrode with Cu and with XC-35, after activation by cycling, is practically the same. The electrode with the additive (Vulcan-XC-72+33% PTFE) showed different behavior. The capacity was much higher in this case, 400 mAh/g versus 320 mAh/g. Figures 3 and 4 also show the influence of additive content on the behavior for MH electrodes. As we have already reported [3], Vulcan - XC-72 as an additive performs better with the hydride electrodes.

Figure 5 shows potential at the end of charge and capacity versus number of cycling at C/3 charge/ discharge behavior of a BNL-4 electrode in 31% KOH solution. The potential and capacity of Figure 5 stays reasonably flat after initial cycling.

Figure 6 compares the discharge capacity as a function of rate of discharge for BNL-4, BNL-11 and BNL-12 hydride materials. The results show that the capacity of BNL-4 does not change very much when discharge current densities increase, however, for two other electrodes the capacity decreases very rapidly with an increase in the rate of discharge.

From these results, it follows that BNL-4 has very high kinetic of hydrogen absorption/desorption which, combined with its excellent capacity, makes it a strong candidate for Ni/MH batteries. The main reason for the big difference between BNL-4 and other tested materials could be its multiphase structure, which according to the model of "Storage and Catalyst Phases", proposed by Gutjar *et al.* [13] allows high storage capacity and reasonable discharge rates.

When a recharged electrode was stored under open-circuit conditions, it was observed that the electrode lost some of its initial capacity with time [14]. Following the capacity measurements discussed in the previous paragraphs, the capacity retention of the best electrode, i.e. BNL-4, was evaluated by allowing a recharged electrode to stay under open-circuit conditions for extended periods of time, followed by discharging at the same rate to monitor the remaining capacity. Figure 7 shows that the capacity remaining in a BNL-4 sample electrode for 300 hours of storage time was 75% of its original, i.e. the self-discharge in 300 hours was less than 25%. The small amount of capacity lost is attributed to the low decomposition pressures and more stable metal-hydride of BNL-4 as shown in P-C-T curves.

Conclusions

Partial substitution of the B element in AB_2 type hydride material (Ovonic) with Co, Mn, Al, and Fe were studied. Comparing the P-C isotherms of all tested materials, we can conclude that Mn increased the plateau pressure,

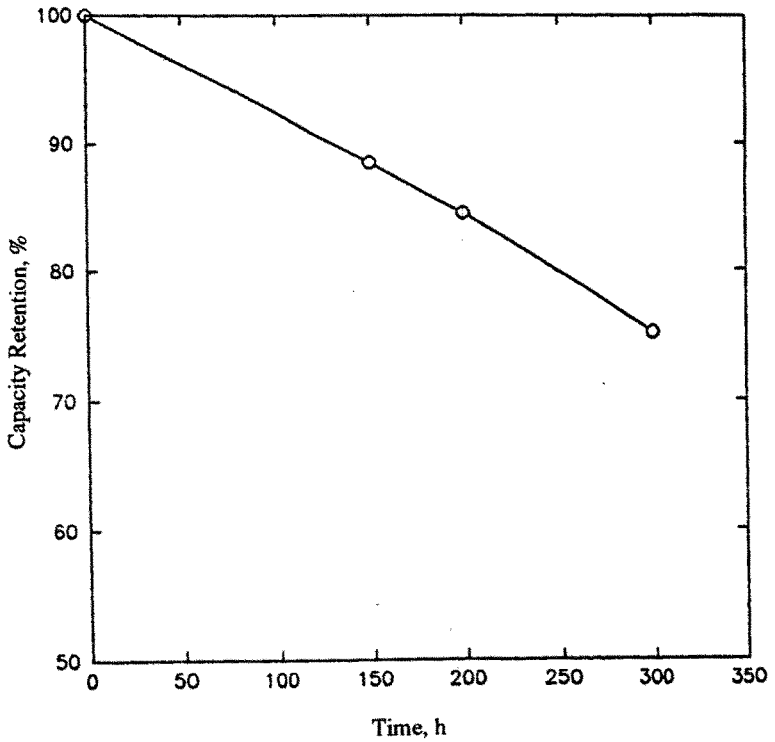

Figure 7. Percentage of capacity retention versus time for BNL-4 active material with XC-35 additive in 8 M KOH solution at

while the addition of small amounts of Al and Fe decreased the plateau pressure. Generally, the addition of all these elements does not improve the gas-phase characteristics of the basic material (Ovonic) BNL-4. BNL-4 has a superior electrochemical capacity, up to 400 mAh/g, as well as high kinetic of hydrogen absorption/desorption, which makes it a strong candidate for Ni/MH batteries. The main reason for the big difference between BNL-4 and other tested materials could be its multiphase structure, which according to the model of "Storage and Catalyst Phases", proposed by Gutjar *et al.* allows high storage capacity and reasonable discharge rates. The small amount of capacity losses is attributed to the low decomposition pressure and the more stable metal-hydride of BNL-4.

References

1. Sakai, T., Yuasa, H. and Ishikawa, H. *J. Less-Common Metals*, **172**, 1194, (1991).
2. Esayed, A. Y. and Northwood, D. O. *Int. J. Hydrogen Energy*, **17**, (1), 41, (1992).
3. Petrov, K., Rostami, A. A., Visintin, A. and Srinivasan, S. *J. Electrochem. Soc.*, **141**, 1747, (1994).
4. Fetcenko, M. A., Venkatesan, S. and Ovshinsky, S. R. *Proc. Chem. Soc.*, **92-5**, 141, (1992).
5. Sandrock, G. D. *et al.* Proc. 2nd World Hydrogen Energy Conf., 1625, (1978).
6. Sakai, T. *et al. J. Electrochem. Soc.*, **137**, 795, (1990).
7. Fetcenko, M. A. *et al.* Ovonic Hydride Battery Technology. IBM Conf. 1726, (1990).
8. Sapru, K. *et al. U. S. Patent*, **4**, 551, (1985).
9. Anani, A. *et al. Proc. Chem. Soc.*, **92-5**, 105, (1992).
10. Matsuok, M., Kdno, T. and Iwakura, *C. Electrochimica Acta*, **38**, (6), 787, (1993).
11. Kahm, K. S. *et al. Int. J. Hydrogen Energy*, **17**, (5), 333, (1992).
12. Niyamura, H. *et al. Proc. Chem. Soc.*, **92-5**, 179, (1992).
13 Gutjar, M. A., Buckner, H., Beccu, K. D. and Saufferrer, H. *Power Sources*, **4**, 79, (1973).
14. Willems, J. J. and Busclow, K. H. *J. Less-Common Metals*, **129**, 13, (1987).